Supplement 2 - Quantifying sample mosaicity

Order parameters and areas in fluid-phase oriented lipid membranes using wide angle x-ray scattering

Thalia T. Mills, Gilman E. S. Toombes, Stephanie Tristram-Nagle, Detlef-M. Smilgies, Gerald W. Feigenson, and John F. Nagle

S2.1   Rocking curves

Fig. S2.1 shows three types of samples: (*A*) a well oriented sample with highly ordered chains, (*B*) a well oriented sample with disordered chains, and (*C*) a poorly oriented sample with highly ordered chains. In Fig. S2.1*C*, the angular distribution of bilayer normal vectors, termed mosaicity, is wide. In Fig. S2.1*B*, the distribution of chain tilt angles is wide. In both of these cases, the chain-chain correlation scattering will have a large angular spread in comparison with the case shown in Fig. S2.1*A*. Since we want the angular spread in the WAXS pattern to indicate the distribution of tilt angles (not the mosaicity), it is important to use well oriented samples for the WAXS experiment. In general, the sample orientation was monitored by observing the mosaic spread of the lamellar repeat peaks along the q_z axis. In well-oriented samples, the Bragg orders are short arcs while in a poorly oriented sample these arcs elongate. In the extreme example of a completely unoriented MLV powder sample, the Bragg peaks become isotropic rings.

Rocking curves provide a quantitative way to obtain mosaic spread. The intensity of a lamellar repeat order is measured as a function of the incident beam angle, α, while holding the scattering angle $2\theta_n$, on the *n*th order peak, fixed. The rocking curve reports the distribution $g(\tau)$ of domains misoriented by the angle $\tau = \alpha - \theta_n$ from perfect orientation $\tau = 0$. Assuming proper alignment of the sample, maximum scattering will occur when $\alpha = \theta_n$:

$$n\lambda = 2D\sin\theta_n . \tag{S2.1}$$

For a rocking curve, the lamellar repeat spacing D must be known and stable. Rocking curves should not be taken on hydrating samples or phase-separated samples. Fig. S2.2 shows two examples of rocking curves for DOPC/DPPC/cholesterol mixtures taken at the D-1 station in February 2006 (plots *B* and *C*) compared with a rocking curve for DMPC taken at D-1 station from a previous Nagle lab experiment (plot *A*) (1). Fig. S2.2*B* was for a sample with WAXS results presented in this paper, and Fig. S2.2*C* was for a sample with WAXS results presented in the accompanying paper (2). We have observed that annealing improves orientation, helping to explain why the samples shown in Fig. S2.2*B*-*C* (samples annealed) have a smaller mosaic spread than in Fig. S2.2*A* (sample not annealed). For Fig. S2.2*B* and *C*, the second lamellar repeat order was used for the measurement. For example, in Fig. S2.2*C* the predicted angle for the maximum intensity was calculated from Eq. S2.1 with $n=2$, $\lambda=1.180$ Å^{-1}, and $D=65.1$ Å^{-1}, giving $\alpha_{max}=1.04°$. Short exposures (less than 1 sec) were then taken for angles above and below α_{max}. Because the minimum exposure time for the shutter was 0.1 sec, a molybdenum attenuator was used to avoid detector saturation near α_{max}. The intensity is integrated for a box surrounding the peak, with care to subtract the specular reflection from silicon, which moves through the

peak as the incident angle is changed. The rocking curves indicate that the samples shown in Fig. S2.2*B* and *C* are well oriented, with sample mosaicities below 0.03° halfwidth at half maximum.
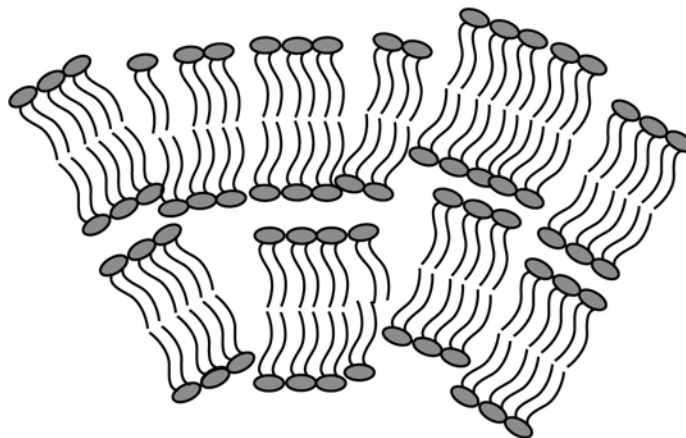
(A) Low mosaicity, high chain orientational order
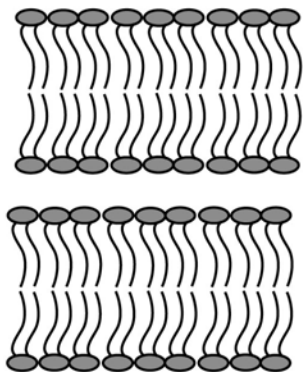
(B) Low mosaicity, low chain orientational order
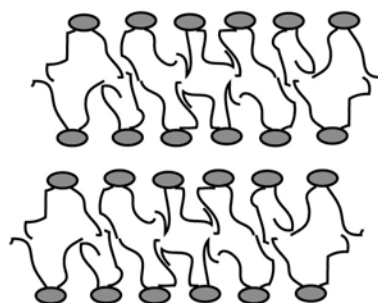
(C) High mosaicity, high chain orientational order

Figure S2.1. Cartoon showing: (*A*) a well oriented sample with highly ordered chains, (*B*) a well oriented sample with disordered chains, and (*C*) a poorly oriented sample with highly ordered chains. In (*B*) and (*C*), the chain-chain scattering will have a larger angular spread in comparison with (*A*).
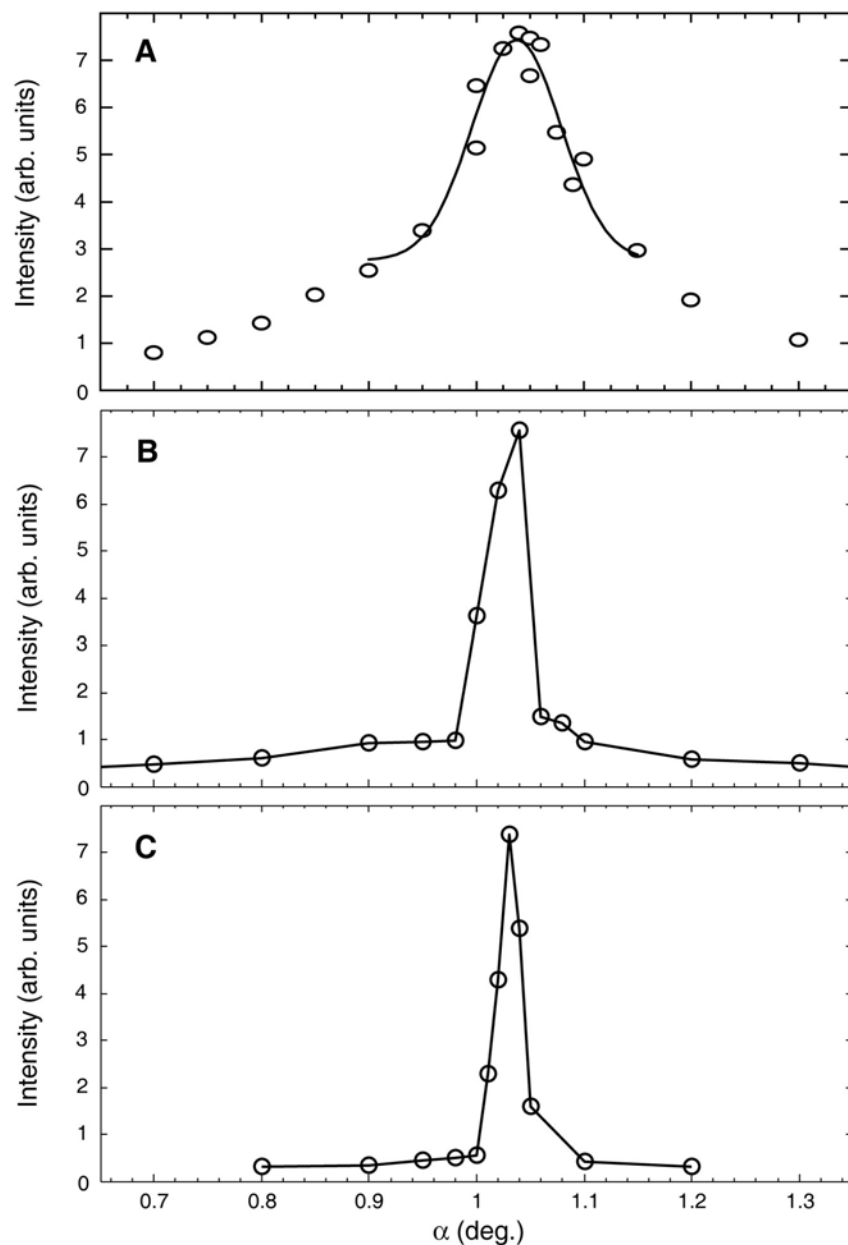
Figure S2.2. Rocking curves showing the intensity of the second lamellar repeat peak vs. α for (*A*) DMPC at 30˚C , (*B*) DPPC + 10% cholesterol at 45˚C, and (*C*) 1:1 DOPC:DPPC + 30% cholesterol at 45˚C. Plot (*A*) is from a previous Nagle lab data (1). In plot (*A*), the black line corresponds to a Gaussian fit, while in (*B*) and (*C*), the black lines connect the points as a guide to the eye. For (*A*), the HWHM from the Gaussian fit is 0.08˚. For (*B*), the intervals in the peaked region are 0.02˚ for α=0.98-1.1˚. These intervals were too large for a good estimate of the HWHM, but we can say that the HWHM<0.03˚ for (*B*). For (*C*), the intervals in the peaked region are 0.01˚ for α=1.0-1.05˚; the HWHM is ~0.01˚.

S2.2 Angular dependence of intensity of lamellar peaks

While rocking curves are often considered to be the gold standard to measure mosaic spread, another way to estimate the orientation of the sample is by examining the angular dependence of the intensity of the lamellar peaks. In Fig. 1 in the main paper, the central portions of the strongest lamellar peaks are attenuated by the beamstop, but scattering from the lamellar mosaicity can still be seen in the lower left-hand corner of the images. Especially in Fig. 1*A*, there appears to be a large mosaic spread based on the angular spread $\gamma=90-\phi$ of the lamellar arcs as well as by the appearance of mosaic scattering from several orders even though the incidence angle was close to zero. However, greyscales can be deceiving. Fig. 1*B* shows the same sample at a different temperature. There is less apparent mosaicity in the h>3 peaks and more in the h=1 and 2 peaks, and these differences are due to the grayscale, which was chosen to emphasize the WAXS data, and the relatively weaker h>3 peaks for fluid phase samples. We also note that there is considerable low angle diffuse scattering in Fig. 1*B* which is important in LAXS structural analysis but is not directly related to mosaicity.

Fig. S2.3 shows lamellar LAXS scattering on a log scale. The sample to detector distance was larger compared with WAXS data collection and the sample was continuously rotated to collect data at all *q* with equal weight. Fig. S2.3*A* is from the same DPPC sample as the WAXS data shown in Figs. 1*A* and *B* in the main paper. Although angular γ spreading of the lamellar arc is visible on the second order peak (q_z~0.2 Å^{-1}) in Fig. S2.3*A*, the intensity falls off rapidly with γ from the peak intensity which is saturated on the CCD detector. The $I(\gamma)$ dependence (γ measured from the q_z axis) is quantified in Fig. S2.4 for the unsaturated intensity of the third order lamellar peak (q_z ~0.3 Å^{-1}) for the two images shown in Fig. S2.3. For each value of γ, the background subtracted intensity was integrated in the radial |*q*| direction over the *q* range corresponding to the full width of the third order peak at half maximum. The values of mosaicity of ~1˚ from this measure, while larger than those obtained from the rocking curves, are too small to be of concern for the analysis of our much broader wide angle data. It may also be noted that the mosaicities are similar for the DOPC and DPPC samples, indicating that the different $S_{\text{x-ray}}$ values obtained for these samples ($S_{\text{x-ray}}=0.44$ for the DPPC sample at 45˚C and $S_{\text{x-ray}}=0.25$ for the DOPC sample at 25˚C) are a result of differences in chain orientation and not in differences in mosaic spread.
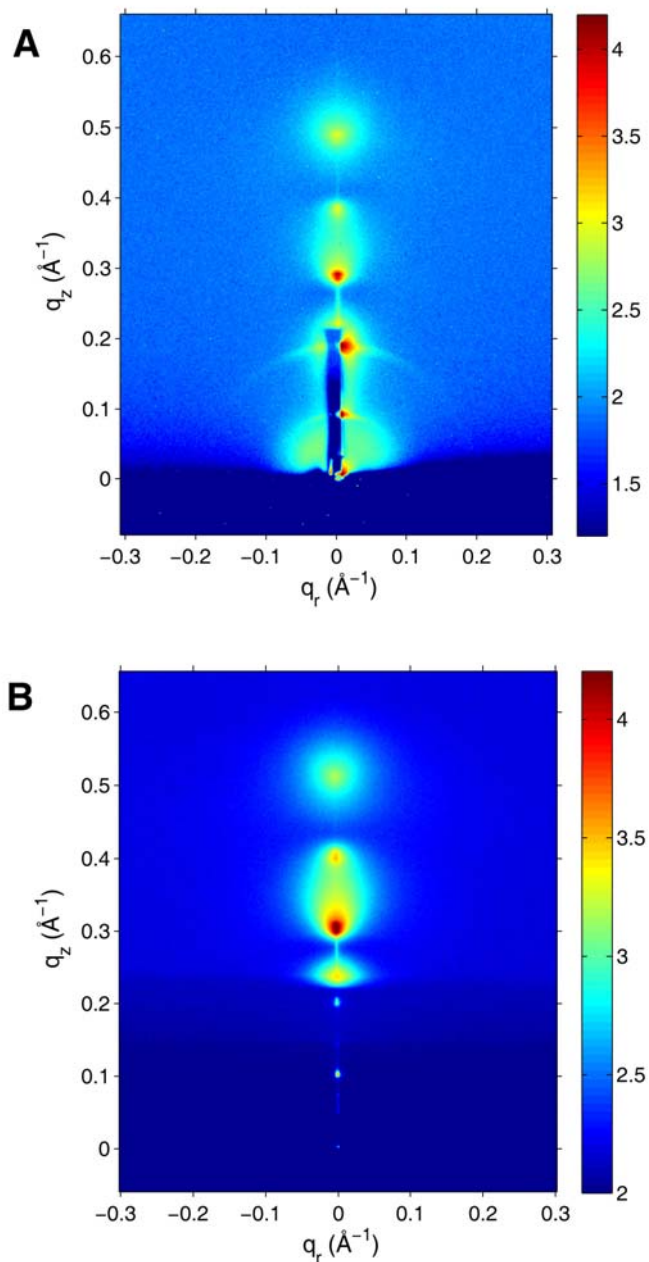
Figure S2.3. 2D CCD images showing the lamellar peaks for (*A*) DPPC at 50˚C and (*B*) DOPC at 30˚C. Intensities are plotted on a logarithmic (base 10) scale. (*A*) shows data from the same sample as for the WAXS data shown in Fig. 1*A* and *B* in the main text of the paper. WAXS data from the sample shown in (*B*) was analyzed and is part of the average results for DOPC shown in Tables 1-3 in the main paper.
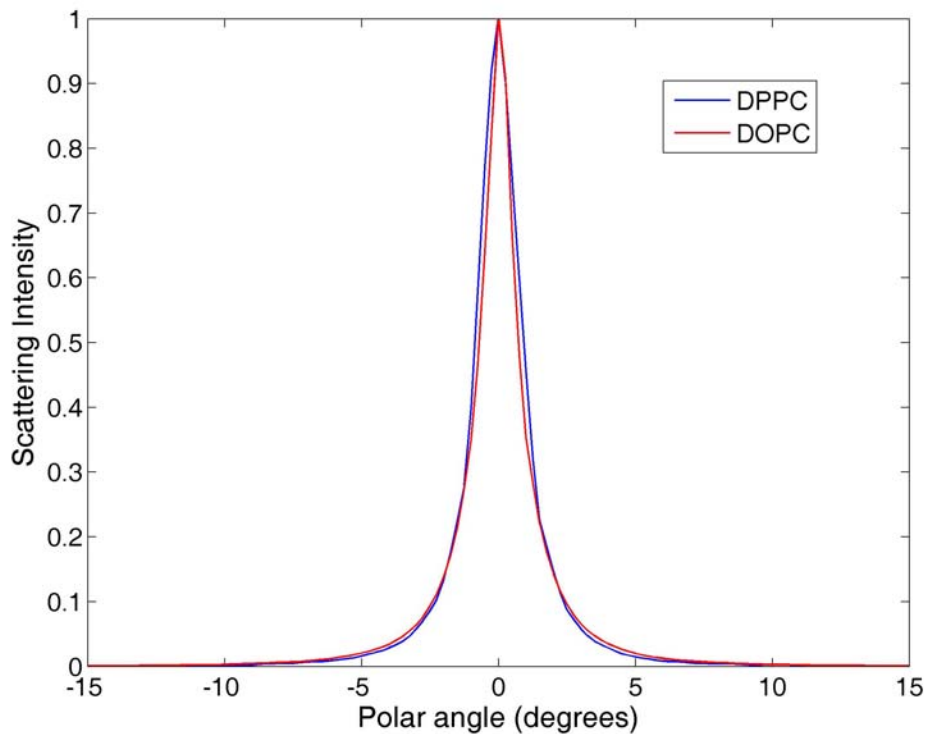
Figure S2.4. Normalized intensity $I(\gamma)$ as a function of polar angle γ for the two images shown in Fig. S2.3. For both images, the q range encompasses the third order lamellar peak (at q_z~0.3 Å-1). Both the DOPC and DPPC plots have a HWHM of approximately 1˚.

REFERENCES

1. Tristram-Nagle, S. 2007. Preparation of oriented, fully hydrated lipid samples for structure determination using x-ray scattering. In Methods in Membrane Lipids. A. M. Dopico, editor. Humana Press, Totowa.
2. Mills, T. T., S. Tristram-Nagle, F. A. Heberle, N. F. Morales, J. Zhao, J. Wu, G. E. S. Toombes, J. F. Nagle, and G. W. Feigenson. 2008. Liquid-liquid domains in bilayers detected by wide angle x-ray scattering. Biophys. J. Submitted.